

# Synthesis and Columnar Mesophase of Fluorescent Liquid Crystals Bearing a $C_2$ -Symmetric Chiral Core

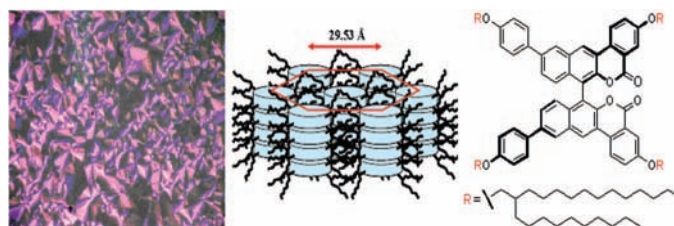
Chia-Wei Yang,<sup>†</sup> Tsai-Hua Hsia,<sup>‡</sup> Cheng-Chung Chen,<sup>‡</sup> Chung-Kung Lai,<sup>\*,‡</sup> and Rai-Shung Liu<sup>\*,†</sup>

Department of Chemistry, National Tsing Hua University, Hsinchu, Taiwan, ROC, and  
Department of Chemistry, National Central University, Chungli, Taiwan, ROC

rsliu@mx.nthu.edu.tw

Received July 11, 2008

## ABSTRACT



A chiral and fluorescent columnar mesogen prepared from chiral binaphthols is reported. This liquid crystal comprises a  $C_2$ -symmetric chiral core with two staggered aromatic planes. Its hexagonal columnar ( $Col_h$ ) mesophase was characterized by appropriate physical methods.

One important objective of synthetic liquid crystal chemistry is to understand the interplay between various elements of design. Chirality is a powerful element for creating novel organizations and functions in liquid crystalline materials.<sup>1</sup> Interesting properties of chiral columnar phases<sup>2</sup> include unique liquid-crystalline structures,<sup>3,4</sup> ferroelectricity,<sup>5</sup> and outstanding second-order nonlinear optical susceptibilities.<sup>6</sup>

Reported chiral columnar liquid-crystalline materials typically comprise a central core with chiral side chains<sup>2</sup> rather than a chiral core bearing regular side chains. The latter examples<sup>7</sup> are limited to derivatives of saccharides,<sup>7a</sup> inositols,<sup>7b</sup> cyclotrimeratrylene,<sup>7c</sup> helicenes,<sup>7d</sup> and metal-containing complexes.<sup>7e</sup>

Although  $C_2$ -symmetric chiral binaphthol and its derivatives served as chiral ligands for asymmetric catalysis,<sup>8</sup> there is no precedent for the use of such chiral building blocks to

<sup>†</sup> National Tsing Hua University.

<sup>‡</sup> National Central University.

(1) Demus, D.; Goodby, J.; Gray, G. W.; Spiess, H.-W.; Vill, V. *Handbook of Liquid Crystals: Fundamentals*; Wiley-VCH: Weinheim, 1998; Vol. 1, Chapter 5.

(2) Recent review for columnar liquid crystals, see: Laschat, S.; Baro, A.; Steinke, N.; Giesselmann, F.; Hagele, C.; Scalia, G.; Judele, R.; Kapatsina, E.; Sauer, S.; Schreivogel, A.; Tosoni, M. *Angew. Chem., Int. Ed.* **2007**, *46*, 4832.

(3) (a) Feng, X.; Pisula, W.; Zhi, L.; Takase, M.; Müllen, K. *Angew. Chem., Int. Ed.* **2008**, *47*, 1. (b) Feng, X.; Pisula, W.; Müllen, K. *J. Am. Chem. Soc.* **2007**, *129*, 14116.

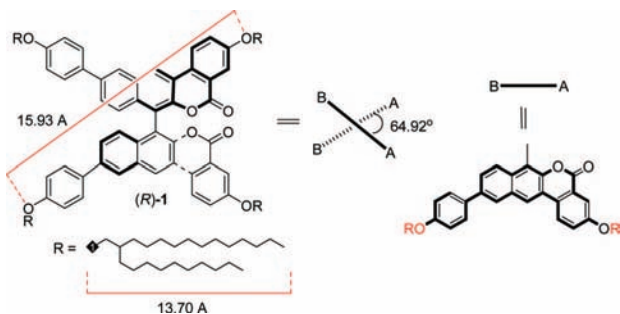
(4) (a) Yelamaggad, C. V.; Achalkumar, A. S.; Rao, D. S. S.; Prasad, S. K. *J. Mater. Chem.* **2007**, *17*, 4521. (b) Percec, V.; Aqad, E.; Peterca, M.; Rudick, J. G.; Lemon, L.; Ronda, J. C.; De, B. B.; Heiney, P. A.; Meijer, E. W. *J. Am. Chem. Soc.* **2006**, *128*, 16365. (c) Barbera, J.; Puig, L.; Romero, P.; Serrano, J. L.; Sierra, T. *J. Am. Chem. Soc.* **2006**, *128*, 4487. (d) Mateos-Timoneda, M. A.; Crego-Calama, M.; Reinhoudt, D. N. *Chem.—Eur. J.* **2006**, *12*, 2630.

(5) (a) Barbera, J.; Iglesias, R.; Serrano, J. L.; Sierra, T.; de la Fuente, M. R.; Palacios, B.; Perez-Jubindo, M. A.; Vazquez, J. T. *J. Am. Chem. Soc.* **1998**, *120*, 2908. (b) Scherowsky, G.; Chen, X. H. *Liq. Cryst.* **1994**, *17*, 803. (c) Bock, H.; Helfrich, W. *Liq. Cryst.* **1995**, *18*, 707. (d) Bock, H.; Helfrich, W. *Liq. Cryst.* **1995**, *18*, 387.

(6) Verbiest, T.; Elshocht, S. V.; Kauranen, M.; Hellemans, L.; Snaawaert, J.; Nuckolls, C.; Katz, T. J.; Persoons, A. *Science* **1998**, *282*, 913. (7) (a) Mukkamala, R.; Burns, C. L., Jr.; Catchings, R. M., III; Weiss, R. G. *J. Am. Chem. Soc.* **1996**, *118*, 9498, and references therein. (b) Kohne, B.; Pracfcke, K. *Angew. Chem., Int. Ed.* **1984**, *23*, 82. (c) Malthête, J.; Collet, A. *J. Am. Chem. Soc.* **1987**, *109*, 7544. (d) Nuckolls, C.; Katz, T. J. *J. Am. Chem. Soc.* **1998**, *120*, 9541. (e) Barberá, J.; Cavero, E.; Lehmann, M.; Serrano, J.-L.; Sierra, T.; Vázquez, J. T. *J. Am. Chem. Soc.* **2003**, *125*, 4527.

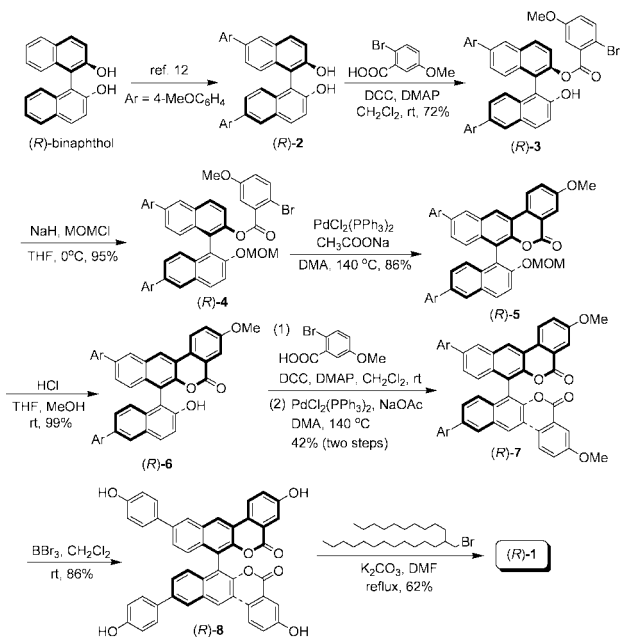
(8) Binap in asymmetric catalysis, see: (a) Knowles, W. S.; Noyori, R. *Acc. Chem. Res.* **2007**, *40*, 1238. (b) Noyori, R. *Angew. Chem., Int. Ed.* **2002**, *41*, 2008.

Scheme 1



prepare chiral liquid crystals. Here we report the first columnar mesogen **1** prepared from chiral binaphthol, which emits fluorescent blue light.<sup>7d,9</sup> Synthesis of such a mesogen is challenging in liquid crystal chemistry because the central core comprises two aromatic planes staggered by 64.92°,<sup>10</sup> which will weaken  $\pi$ - $\pi$  interactions. To circumvent this issue, compound **1** is designed to have two lactone rings, which might stabilize columnar aggregates through dipole-dipole interactions.<sup>11</sup>

Scheme 2. Synthetic Route toward (R)-1



Scheme 2 depicts the preparation of key building block (R)-2 from (R)-binaphthol according to literature procedures.<sup>12</sup> Treatment of species (R)-2 with 2-bromo-5-

(9) Very few examples are known for chiral fluorescent liquid crystals. See ref 7d: Fechtenkötter, A.; Tehebotareva, N.; Watson, M.; Müllen, K. *Tetrahedron* **2001**, *57*, 3769.

(10) Theoretical calculation for dihedral angle by a Silicon Graphics O2+ workstation. The programs Builder and Biopolymer were used for the construction of structures. The program Discover was used for the maximum derivative which was less than 1.0 kcal mol<sup>-1</sup> Å<sup>-1</sup>.

methoxybenzoic acid, *N,N*-dicyclohexylcarbodiimide (DCC), and 4-(dimethylamino)pyridine (DMAP) in equimolar proportions afforded ester (R)-3 in 72% yield. After conversion of the remaining hydroxyl to a methoxymethyl ether, Mizoroki–Heck coupling of species (R)-4 with PdCl<sub>2</sub>(PPh<sub>3</sub>)<sub>2</sub> at 140 °C provided compound (R)-5 bearing a single lactone. After acid-catalyzed hydrolysis of the methoxymethyl ether of compound (R)-5, the resulting alcohol (R)-6 was subject to a second esterification and Mizoroki–Heck coupling,<sup>13</sup> giving desired bislactone compound (R)-7. Subsequent treatment of compound (R)-7 with BBr<sub>3</sub>, followed by alkylation with 2-decyl-tetradecylbromide and K<sub>2</sub>CO<sub>3</sub> gave final product (R)-1 [R = CH<sub>2</sub>CH(C<sub>12</sub>H<sub>25</sub>)C<sub>10</sub>H<sub>21</sub>]. We reluctantly chose this large racemic alkyl substituent after we were unsuccessful in obtaining similar compounds containing a long alkyl (R = C<sub>12</sub>H<sub>25</sub>) and short branched alkyl (R = CH<sub>2</sub>CH(C<sub>2</sub>H<sub>5</sub>)C<sub>6</sub>H<sub>13</sub>) groups because of a solubility problem. The long branched alkyl substituent of (R)-1 is considered to have pseudo-C<sub>5</sub> symmetry because of similar electronic properties between the decyl and octyl groups. This hypothesis is supported by the same magnitude of optical rotations of (R)-1 ([ $\alpha$ ]<sub>D</sub><sup>23</sup> = -57.2. *c* = 0.2, CHCl<sub>3</sub>) and its enantiomer (S)-1 forms ([ $\alpha$ ]<sub>D</sub><sup>23</sup> = +56.9. *c* = 0.2, CHCl<sub>3</sub>). Furthermore, <sup>1</sup>H and <sup>13</sup>C NMR spectra of (R)-1 only reveal signals of one species for both the central core and side chains despite the presence of eight diastereomers. Compound (R)-1 is fairly soluble in common organic solvents, including THF, hexane, toluene, and dichloromethane and can thus be purified on a short column and subsequent recrystallization from CH<sub>2</sub>Cl<sub>2</sub>/EA. We prepared its enantiomer (S)-1 using (S)-binaphthol as a starting reagent.

The UV–vis absorption of compound (R)-1 is shown in Figure 1. In CH<sub>2</sub>Cl<sub>2</sub> (1.0 × 10<sup>-5</sup> M), compound (R)-1 showed

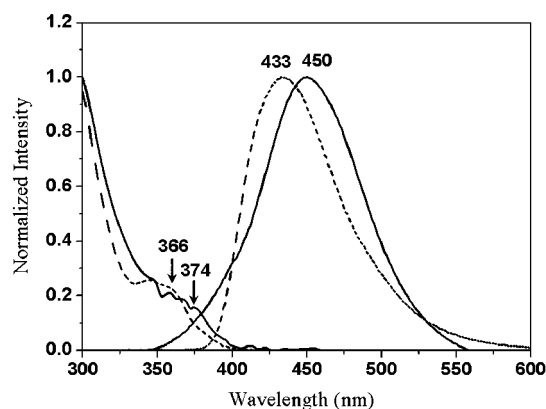
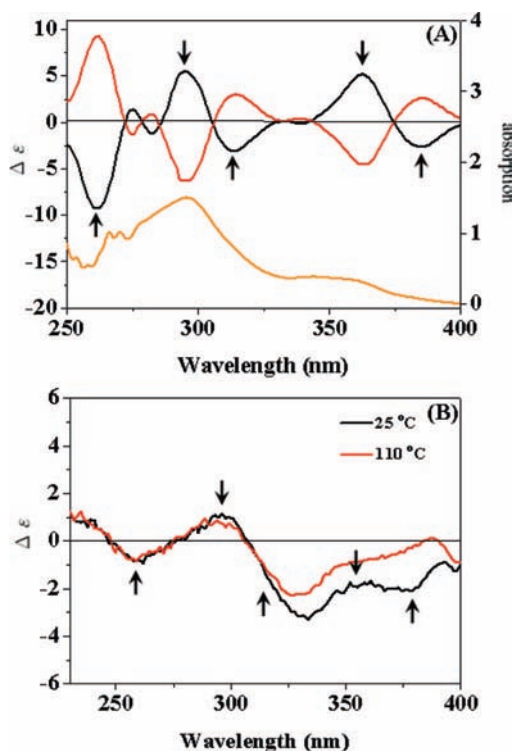


Figure 1. Absorption and emission spectra of compound (R)-1 in dichloromethane solution (dash), in a thin film (solid).

an absorption maximum at 366 nm in the 300–450 nm region. The absorption maximum of (R)-1 as a thin film occurred at 373 nm, a red shift ca. by 8 nm. The photoluminescence spectra (PL) of (R)-1 as a thin film showed an

emission maximum at 450 nm, a red shift ca. 17 nm from that (433 nm) of the solution state ( $\text{CH}_2\text{Cl}_2$ ,  $1.0 \times 10^{-5}$  M). The quantum yields of (*R*)-**1** in  $\text{CH}_2\text{Cl}_2$  and a thin film were 0.15 and 0.05 at 28 °C, respectively. We estimated the HOMO energy level ( $-5.70$  eV) from their oxidation potentials ( $E_{1/2\text{ox}}$ ) and obtained the LUMO absorptions.

In the circular dichroism (CD) spectra of (*S*)- and (*R*)-**1** in  $\text{CH}_2\text{Cl}_2$  ( $1 \times 10^{-5}$  M), maxima associated with the  $n-\pi^*$  and  $\pi-\pi^*$  transitions were observed at 295 and 366 nm, respectively, by comparison to their UV-vis absorptions (Figure 2).<sup>14</sup> In the case of (*R*)-**1**, two negative exciton



**Figure 2.** (A) CD spectra of (*R*)-**1** (black line) and (*S*)-**1** (red line) in  $\text{CH}_2\text{Cl}_2$  ( $1 \times 10^{-5}$  M) and UV absorption spectra of (*R*)-**1** (orange line) in  $\text{CH}_2\text{Cl}_2$  ( $1 \times 10^{-5}$  M). (B) CD spectra of (*R*)-**1** in thin film at 25 °C (black line) and 110 °C (red line), respectively; the arrows represent the original maxima and minima of the solution CD.

couplings are observed ( $\Delta \epsilon_{385}^{\text{max}} = -2.7$ ,  $\Delta \epsilon_{362}^{\text{max}} = +5.2$ , and  $\Delta \epsilon_{314}^{\text{max}} = -3.1$ ,  $\Delta \epsilon_{295}^{\text{max}} = +5.2$ ) for these two transitions because (*R*)-**1** has two staggered planar chromophores. In contrast, (*S*)-**1** showed opposite signs to the CD curves of (*R*)-**1**. These CD curves clarify the enantiomeric relations between (*R*)-**1** and (*S*)-**1** on their central chiral chromophores. We measured the CD spectra of (*R*)-**1** in thin film at 25 and 110 °C at which the Col-phase was observed (vide ante). Although these CD curves retain the characteristic peaks of the solution state including the excited coupling ( $\lambda_{\text{max}} = 295$  nm,  $\lambda_{\text{min}} = 314$  nm), the peaks ( $\lambda_{\text{max}} = 362$  nm,  $\lambda_{\text{min}} = 385$  nm) were very weak at 25 °C and disappeared at 110 °C. We did not observe a new and intensive exciton splitting assignable to a chiral helical columnar suprastructure in the

CD curves. Instead, the loss of exciton coupling in the 330–400 nm region suggests that electric dipole moments generated in  $\pi-\pi^*$  transitions from the neighboring chromophores are parallel to each other to give no optical activity.<sup>14</sup> Notably, the excitation coupling is still recognizable for the  $n-\pi^*$  transition in thin film. This information is helpful to understand the nature of molecular stacking of species (*R*)-**1** into the hexagonal columnar suprastructure.<sup>15</sup>

Compound (*R*)-**1** was truly mesogenic based on DSC analysis and polarized microscopy. The DSC analysis (Table 1) at a scan rate of  $10^{-1}$  showed a typical columnar phase

**Table 1.** Phase Behavior of (*R*)-**1**<sup>a</sup>

compound	behavior	
( <i>R</i> )- <b>1</b>	Cr $\xrightleftharpoons[95.0^b]{105.6 (1.76)}$ Col <sub>ho</sub>	Col <sub>ho</sub> $\xrightleftharpoons[195.1 (2.10)]{202.9 (2.21)}$ I

<sup>a</sup> The units of transition temperature and transition enthalpies are °C and kJ/mol by DSC at a scan rate of 10 °C/min. <sup>b</sup> Determined by an optical microscope.

transition, crystal to columnar to isotropic (Cr→Col→I). The mesophase was identified as an ordered hexagonal columnar phase (Col<sub>ho</sub>), and the temperature range for the Col-phase was notably wide although the central core comprises two staggered fused aromatic rings. In addition, a moderate enthalpy ( $\Delta H = 2.21$  kJ/mol on heating cycle) for the Col<sub>ho</sub>→I transition was observed. The transition temperature for Col→Cr was not observed with DSC but was clearly shown with optical microscopy. Under polarized optical microscopy, upon heating, the material melted to give a birefringent fluid phase with columnar superstructures, and we observed a large area of domains displaying prominent wedge-shaped defects or focal-conic patterns (Figure 3).

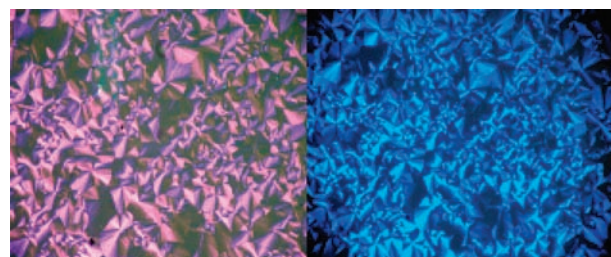


**Figure 3.** Optical textures observed: Col<sub>ho</sub> phase at 194.0° (left plate) and Cr phase at 100.0° (right plate).

A powder X-ray diffraction experiment confirmed the hexagonal columnar (Col<sub>h</sub>) phases. A typical pattern of one strong (25.57 Å) and two weaker features (14.79 Å & 12.84 Å) at small angles and one diffuse broad peak (4.89 Å) at a large angle were observed with a spacing ratio of 1:(1/3)<sup>1/2</sup>:1/2. The diffraction pattern (Figure 4) pertains to a Col<sub>h</sub>

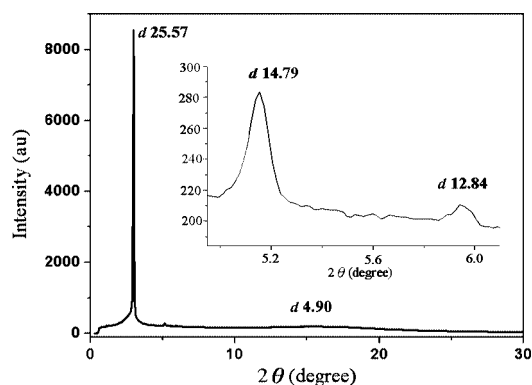


**Figure 4.** Powder X-ray diffraction pattern of compound (*R*)-**1** at 170 °C.

columnar arrangement,<sup>2,16</sup> corresponding to (10), (11), and (21), giving a lattice parameter of 29.53 Å. The XRD experiment obtained at 50 °C was similar to that at 170 °C, indicating the phase structure was also similar. The interdisk distance showing the more ordered packing within the columns, often occurring at ca. 3.0~3.3 Å, was not observed, which might overlap with the broad halo peak.

The distance (29.53 Å) between two column centers suggests that each column consists of a stacking of a single molecule of (*R*)-**1** rather than its dimer, and the structural protocol is shown in Figure 5. The distance outside the two hard cores, ca. 13.60 Å, is close to the maximum length of one side chain (13.70 Å). With IR spectra of species (*R*)-**1** in nujol, we only observed the strong  $\nu(\text{C}=\text{O})$  stretching of ester (1748  $\text{cm}^{-1}$ ), whereas the  $\nu(\text{O}-\text{H})$  band of water (3600–3300  $\text{cm}^{-1}$ ) was undetectable. Accordingly, molecular assembly of species (*R*)-**1** into a columnar structure relies primarily on intermolecular dipole–dipole interaction. We propose a head-to-tail stacking model of (*R*)-**1** such that each column can be maintained with zero dipole moment. This molecular packing also rationalizes our CD results that exciton coupling is more pronounced for the  $n-\pi^*$  transition than for the  $\pi-\pi^*$  transition in liquid crystal phases. In the head-to-tail stacking, the electric dipole moment generated in the  $n-\pi^*$  transition is not parallel to those of the two

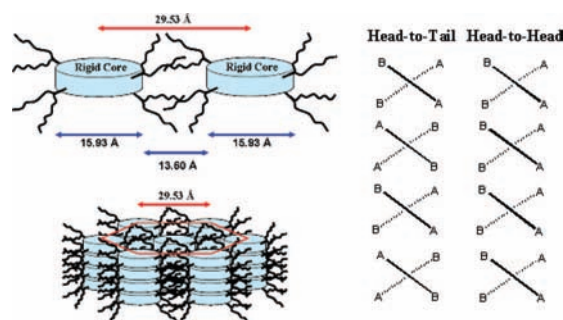


**Figure 5.** Hexagonal columnar ( $\text{Col}_h$ ) mesophase and molecular stacking models for (*R*)-**1** (see Scheme 1 for a structural representation of B-A).

neighboring molecules, whereas the corresponding  $\pi-\pi^*$  charge transition has the parallel relations with the two proximate molecules. In the case of the head-to-head packing mode, we envision that both  $n-\pi^*$  and  $\pi-\pi^*$  transitions will lose excitation coupling in thin-film CD spectra. A detailed analysis of these charge transitions is provided in the Supporting Information.

In summary, we report a chiral and fluorescent columnar mesogen (*R*)- and (*S*)-**1** prepared from chiral binaphthols. This liquid crystal comprises a  $C_2$ -symmetric chiral core<sup>17,18</sup> with two aromatic planes staggered by a large angle (64.92°). Its hexagonal columnar ( $\text{Col}_h$ ) mesophase was characterized by appropriate physical methods, and the CD spectra indicate that molecular packing of (*R*)-**1** follows a head-to-tail stacking mode. We envisage that this atypical mesogen will be helpful in the design of new chiral and fluorescent liquid crystals for future optical applications.

**Acknowledgment.** The authors wish to thank the National Science Council, Taiwan, for supporting this work.

**Supporting Information Available:** Analysis of charge transitions for molecular packing, detailed synthesis, cyclic voltammogram, spectral data, NMR spectra, and MALDI-TOF mass spectra of compound (*R*)- and (*S*)-**1**. This material is available free of charge via the Internet at <http://pubs.acs.org>.

OL801561B

(11) (a) Jones, B. A.; Facchetti, A.; Wasielewski, M. R.; Marks, T. J. *J. Am. Chem. Soc.* **2007**, *129*, 15259. (b) Foster, E. J.; Jones, R. B.; Lavigne, C.; Williams, V. E. *J. Am. Chem. Soc.* **2006**, *128*, 8569. (c) Debije, M. G.; Chen, Z. J.; Piris, J.; Neder, R. B.; Watson, M. M.; Müllen, K.; Würthner, F. *J. Mater. Chem.* **2005**, *15*, 1270. (d) Eichhorn, S. H.; Paraskos, A. J.; Kishikawa, K.; Swager, T. M. *J. Am. Chem. Soc.* **2002**, *124*, 12742. (e) Kishikawa, K.; Furusawa, S.; Yamaki, T.; Kohmoto, S.; Yamamoto, M.; Yamaguchi, K. *J. Am. Chem. Soc.* **2002**, *124*, 1597.

(12) Chen, R.; Qian, C.; de Vries, J. G. *Tetrahedron Lett.* **2001**, *42*, 6919.

(13) Ames, D. E.; Opalko, A. *Tetrahedron* **1984**, *40*, 1919.

(14) Lightner, D. A.; Gurst, J. E., *Organic Conformational Analysis and Stereochemistry from Circular Dichroism Spectroscopy*; Wiley-VCH: Weinheim, 2000; Chapter 14.

(15) After the CD measurement, the used sample (*R*)-**1** of thin film has  $[\alpha]_D^{23} = -56.2$ . ( $c = 0.2$ ,  $\text{CHCl}_3$ ) very close to that ( $[\alpha]_D^{23} = -57.2$ ) of the authentic sample. This information shows negligible loss of enantiopurity, and even the sample was pretreated at 110 °C.

(16) Fontes, E.; Heiney, P. A.; Ohba, M.; Haseltine, J. N.; Smith, A. B., III. *Phys. Rev. A.* **1988**, *37*, 1329.

(17)  $C_2$ -symmetric chiral compounds were often used as a dopant 18 rather than a building block to form liquid crystals.<sup>7e</sup>

(18) (a) Boulton, C. J.; Finden, J. G.; Yuh, E.; Sutherland, J. J.; Wand, M. D.; Wu, G.; Lemieux, R. P. *J. Am. Chem. Soc.* **2005**, *127*, 13656. (b) Pijper, D.; Jongejan, M. G. M.; Meetsma, A.; Feringa, B. L. *J. Am. Chem. Soc.* **2008**, *130*, 4541.